Optics Communications 358 (2016) 120–125

Contents lists available at ScienceDirect

Optics Communications

journal homepage: www.elsevier.com/locate/optcom

Analysis on laser-induced transient damage behavior in multilayer coating

Du Lifeng [a], Fu Bo [b], Li Fengyu [a], Zhang Rongzhu [a,*]

[a] College of Electronics and Information Engineering, Sichuan University, Chengdu 610064, China
[b] Institution of Fluid Physics, China Academy of Engineering Physics, Mianyang 621900, Sichuan, China

ARTICLE INFO

Article history:
Received 15 May 2015
Received in revised form
2 September 2015
Accepted 3 September 2015
Available online 19 September 2015

Keywords:
Anti-reflective coating
Avalanche ionization
Complex refractive index

ABSTRACT

Based on the ionization theory and the Drude model of free electron gas, transient damage principle of the anti-reflection coating under ultrashort pulses are analyzed. Specifically, the damage of an anti-reflection coating designed by ZnS/SiO_2 materials is calculated. The results show that during the irradiation process the parameters, such as the refractive index, the electric field and the free electron density, should impact on each other. The coupling relationship between these parameters causes the change in the refractive index, which further leads to the decrease of transmittance of anti-reflection coating from 0.96 to 0.01. In addition, the coupling relationship causes the repartition of free electron density constantly, which eventually leads to the external damage of anti-reflection coating.

1. Introduction

Multilayer coatings are applied to many optical elements to improve the optical properties. Unfortunately, they are the weakest part in an optical system when laser damage resistance is concerned. Their damage resistance will directly affect the application of entire optical system. With the rapid development of ultra-short pulse technology, more strict requirements are put forward on the laser damage resistance of multilayer coatings due to the highly concentrated energy in time domain. Therefore, to analyze the damage characteristics of multilayer coatings is meaningful for improving the damage threshold of whole optical system.

With the development of chirped pulse amplification (CPA), studies of damage under ultra-short laser pulses are carried out. In 1990s, using the impact ionization and photoionization theory, Du and Stuart analyzed the nanosecond-to-femtosecond laser-induced breakdown in fused silica [1–3]. Subsequent damage researches are carried out in multilayer films with the impact ionization and photoionization theory. Among these damage researches of films, the damage threshold dependence of electric field has aroused great interest [4–8]. And a latest development of researches is the considering of electric field repartition when calculating the damage threshold [9]. Specifically, Laurent Gallais pointed out that the growth of free electrons induced by ultra-short pulse will cause change in the refractive index, which will lead to repartition of the electric field. Therefore, the refractive index correction should be considered when calculating the damage threshold.

The previous studies of laser-induced damage of multilayer coating is mainly focused on high-reflection coating, rarely focused on antireflection coating. In the most detection system, multilayer coating is served as antireflection coating to improve response of optical detection system. During the irradiation of an ultra-short laser pulse, the strong incident electric field will increase the number of free electrons by photoionization and avalanche ionization. The growth of free electron density will change the refractive index of materials. These changes in complex index will lead to modifications of the electric field repartition, and further lead to variation in the free electron density [10–11]. In this paper, given the basic characteristics of ZnS and SiO_2 materials [12], a study on antireflection coating designed by ZnS/SiO_2 materials is carried out. The variation of the free electron density has been calculated. Meanwhile, the correction of refractive index and the modifications of the normalized electric field intensity during the above process have been analyzed in detail.

2. Basic theory

2.1. The breakdown of material induced by avalanche ionization and photoionization

When irradiated by ultra-short laser pulses, the electrons in dielectric media can be excited up to the conduction band via avalanche ionization and photoionization. The free-electron

* Corresponding author.
E-mail address: zhang_rz@scu.edu.cn (Z. Rongzhu).

http://dx.doi.org/10.1016/j.optcom.2015.09.010
0030-4018/

generation in dielectrics can be described as [10]:

$$\frac{d\rho(t,Z)}{dt} = (R_{PI} + R_{AI}\rho)(1-\rho/\rho_1) \tag{1}$$

Where $\rho(t)$ is the free electron density in conduction band. The factor $1-\rho/\rho_1$ is the exhaust of valence electrons. ρ_1 is the initial density of valence electron. R_{AI} is the electron avalanche rate [13], R_{PI} is the photo-ionization rate calculated by Keldysh theory [14,15].

Combined with the initial condition of $\rho(t=0)=\rho_0$, the variation of free electron density can be calculated by solving Eq. (1). The parameters used in the calculation of photo-ionization rate and electron avalanche rate are shown in Table 2.

With the increasing of irradiation time t, the free electron density of dielectric media accumulates. When the density accumulates to critical value ρ_c, the phenomenon of plasma flash appears with the dielectric constant of materials mutating. As a result of the plasma flash, the material's refractive index increases and transmittance decreases quickly. This phenomenon is regarded as the symbol of laser-induced damage in dielectric media.

2.2. Calculation of electric field in multilayer coating

In Eq. (1), R_{AI} and R_{PI} are both functions of electric field E. Therefore, it is necessary to calculate the electric field distribution of multilayer coating by Maxwell's equations.

Fig. 1 shows an X-1-layer structure which is irradiated by laser pulse. Starting at the substrate with $k=1$, the layers are numbered in increasing order. The kth layer has thickness z_k, refractive index n_k. The laser is propagating through the multilayer coating in the direction of Z. Based on the Maxwell equations, the electric field $E_k(Z)$ and the magnetic field $H_k(Z)$ in Fig. 1 are calculated by Eqs. (2) and (3) [16].

$$E_k(Z) = A_1^{(k)}(\exp\{-i[2\pi n^{(k)}/\lambda_0](Z-\sum_{j=k+1}^{X+1} z_j)\} + A_2^{(k)}\exp\{+i[2\pi n^{(k)}/\lambda_0](Z-\sum_{j=k+1}^{X+1} z_j)\}) \tag{2}$$

$$H_k(Z) = n^{(k)}A_1^{(k)}(\exp\{-i[2\pi n^{(k)}/\lambda_0](Z-\sum_{j=k+1}^{X+1} z_j)\} - A_2^{(k)}\exp\{+i[2\pi n^{(k)}/\lambda_0](Z-\sum_{j=k+1}^{X+1} z_j)\}) \tag{3}$$

In the above equations, take the thickness of air layer z_{X+1} as zero. Coefficients $A_1{}^{(k)}$ and $A_2{}^{(k)}$ are determined by refractive index and thickness of the kth layer. $A_2{}^{(k)}$ can be given below:

$$A_2^{(k)} = \downarrow\frac{[n^{(k)}-n^{(k-1)}]/[n^{(k)}+n^{(k-1)}] + A_2^{(k-1)}}{1+\{[n^{(k)}-n^{(k-1)}]/[n^{(k)}+n^{(k-1)}]\}A_2^{(k-1)}} \downarrow\times \exp\{-i[4\pi n^{(k)}/\lambda_0]z_k\}\, 2 \le k \le X+1 \tag{4}$$

Since the reflected component of light in the substrate is zero, we can start with $A_2{}^{(1)}=0$. Other A_2 can be calculated successively from Eq. (4). Once the coefficients A_2 are calculated, we can obtain A_1 according to the theory of continuity of the electric field.

$$A_1^{(k)} = \downarrow\frac{\exp\{-i[2\pi n^{(k+1)}/\lambda_0]z_{k+1}\}}{1+A_2^{(k)}} \downarrow+\frac{A_2^{(k+1)}\exp\{-i[2\pi n^{(k+1)}/\lambda_0]z_{k+1}\}\}}{1+A_2^{(k)}} \times A_1^{(k+1)}\, 1 \le k \le X \tag{5}$$

$A_1{}^{(X+1)}$ is the incident light amplitude.

By solving Eqs. (2)–(5), $E_k(Z)$ can be calculated recursively. For applying to multilayer coating Eq. (1) can be rewritten as:

$$\frac{d\rho^k(t,Z)}{dt} = (R_{PI}^k + R_{AI}^k\rho^k)(1-\rho^k/\rho_1) \tag{6}$$

2.3. The correction theory of refractive index

When the free electron density reaches values of 10^{21} cm^{-3}, such electronic densities strongly affect the dielectric function of the material under irradiation. According to the Drude model of free electron gas, the complex refractive index dependence of electronic density can be described below:

$$N(\rho) = \sqrt{n^2 - \frac{\rho e^2}{m\varepsilon_0(\omega^2 + i\omega/\tau_D)}} \tag{7}$$

Where n is the refractive index of the unexcited material, ε_0 is the free space dielectric permittivity, τ_D is the Drude relaxation time with the value of 10^{-15} s [17].

A strong incident electric field will increase the number of free electrons by photoionization and avalanche ionization. The growth of free electron density will change the refractive index of materials. These changes in complex index will lead to modifications of the electric field repartition, and further lead to variation in the free electron density. Considering the complexity of this process, we take the iterative method to calculate the spatial and time distribution of the coupling parameters: Firstly, calculate the initial electric field of antireflection coating by Eqs. (2)–(5).Secondly, calculate the free electron density by Eq. (6).Thirdly, calculate the complex index by Eq. (7). Finally, solve the process iteratively according to the above order. Each iteration time is set to Δt. The process continues until the end of the pulse irradiation.

3. The simulation and analysis

Based on the analyses model introduced above, an anti-reflective coating is employed as the object of study. The anti-reflective coating is a finished product used in a custom-builted detector. And the design of anti-reflective coating is offered by the detector provider.The design parameters are given in Table 1. Table 2 shows the relevant parameters of SiO_2 and ZnS to calculate the free electron density [1,13,18,19].

The incident laser is a Gaussian pulse with wavelength of 650 nm and pulse width of 50 fs, as shown in Fig. 2. The total energy density of laser pulse is 0.18 J/cm^2.The parameter "0.18 J/cm^2" is not based on a practical damage measurement but the theoretical calculations result, which we have verified

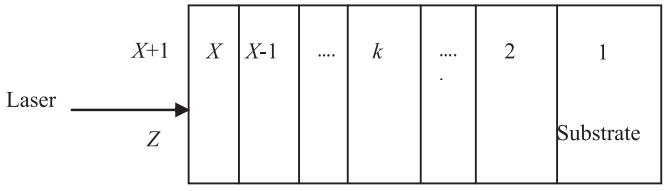

Fig. 1. The model of multilayer coating with laser irradiation.

Table 1
Design parameters of the anti-reflective coating.

Film stack	λ/nm	n
G/0.7320L(1.4639H1.4641L)^7 (1.4639H1.3420L)(1.22H1.22L)^7 (1.22H0.6101L)/A	650	H–ZnS,2.35 − i2.7 × 10^{-4} L-SiO_2,1.46–i2 × 10^{-4} G-glass,1.52

Table 2
Thermodynamics parameters of the constituent materials.

Parameter	Material	
	SiO_2	ZnS
Band gap E_g	7.8 eV	3.7 eV
Effective electron mass m	$0.5 \times 9.11 \times 10^{-31}$ kg	$0.28 \times 9.11 \times 10^{-31}$ kg
Initial free electron density ρ_0	1×10^{10} cm^{-3}	1×10^{10} cm^{-3}
Saturated free electron density ρ_c	1.6×10^{21} cm^{-3}	2.2×10^{22} cm^{-3}
Initial density of valence electron ρ_1	2.2×10^{21} cm^{-3}	2.2×10^{21} cm^{-3}
Relative dielectric constant ε	$4 \times 8.85 \times 10^{-12}$	$8.2 \times 8.85 \times 10^{-12}$
Electron impact relaxation time τ	0.1 ns	0.1 ns
Diffusion and recombination relaxation time (τ_D,τ_R)	10 ns	10 ns
Electron saturated drift velocity v_s	2.0×10^5 m/s	2.0×10^5 m/s
Field strength to overcome ionization scattering E_I	30 MV/m	30 MV/m
Field strength to overcome phonon scattering E_P	3.2 MV/m	3.2 MV/m
Field strength to overcome thermal scattering E_{KT}	0.01 MV/m	0.01 MV/m

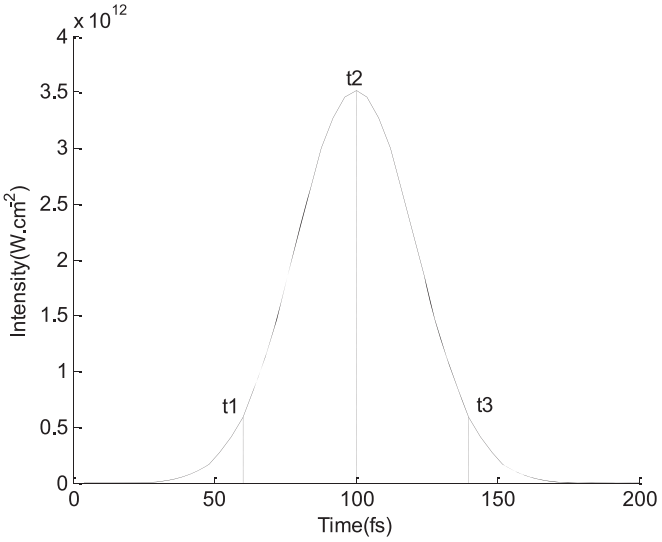

Fig.2. Schematic profile of single 650 nm, 50 fs laser pulse in the simulation with three different moments marked by $t1$, $t2$, and $t3$.

repeatedly. According to our calculation results, the film will be damaged when the laser fluence is 0.18 J/cm^2 [10,20]. Each iteration time is set to 1 fs. In order to analyze the space-time variations of coupling parameters in the process of damage, three different moments of 60 fs, 100 fs and 140 fs are concerned. The three moments, which marked by $t1$, $t2$, and $t3$, correspond to the initial, peak, and terminative intensity of laser pulse, respectively. Note that the above works are simplified for calculating easily, regardless of the interfaces in antireflection coating.

Fig. 3 shows the free electron density, complex index and normalized electric field intensity within the antireflection coating when $t=0$, 60 fs, respectively. The grey stripe shows SiO_2, while white stripe shows ZnS. As shown in Fig. 3(a), the initial free electron density is 10^{10} cm^{-3} when $t=0$. Then the free electron density accumulates little after 60 fs. The maximum of free electron density is 6×10^{19} cm^{-3}, which located in the Layer 25 of the antireflection coating. In addition, the free electron density in ZnS layer is much greater than which in SiO_2 layer due to the higher photoionization rate of ZnS. Fig. 3(b)–(c) is the real and imaginary parts of the complex index, respectively. The real part of refractive index at the moments of $t=0$ and $t=60$ fs are completely equal, while the imaginary part of refractive index has a slight increase from 0 to 2.2×10^{-3}. Obviously, the refractive index remains almost unchanged, for the electronic density is not strong enough to affect the dielectric function during 60 fs. Note that the absorption of material is characterized by the imaginary part. Fig. 3(d) shows the normalized electric field intensity at the moments of $t=0$ and $t=60$ fs are completely equal. The maximum is located in the Layer 26 of antireflection coating.

When $t=100$ fs, the maximum of free electron density accumulates to a value of 4.5×10^{21} cm^{-3}. The maximum is located in the Layer 27 of the antireflection coating (Fig.4(a)). The electronic density is too strong to affect the dielectric function at this moment. Consequently, the real part of complex refractive index has decreased obviously, while the imaginary part has increased to 0.28 (Fig.4(b)–(c)). These changes in complex index lead to further modifications of the electric field repartition. The location of maximum of normalized electric field intensity moves to Layer 30 of antireflection coating after the repartition process (Fig.4(d)).

The pulse irradiation ends at the moment of $t=140$ fs. Fig. 5 (a) shows that the maximum of free electron density accumulates to 2.3×10^{22} cm^{-3}. The maximum is located in the Layer 33 of antireflection coating. According to the damage criterion, the antireflection coating is considered to be damaged because the free electron density in Layer 33 reaches the critical value of 10^{22} cm^{-3}. At the moment, the complex refractive index has mutated due to the large accumulation of free electrons. The real part of complex refractive index has decreased to 0.75, while the imaginary part has increased to 3.6 (Fig.5(b)–(c)). The location of maximum of normalized electric field intensity moves to Layer 34 of antireflection coating after a further repartition (Fig.5(d)).

Summarily, the maximums of normalized electric field intensity and free electron density are moving toward the air/film interface in the coupling process. The damage has occurred in Layer 33 eventually.

For the antireflection coating, the change of complex index of each layer will lead to the variation of the transmittance. Fig. 6 shows the transmittance curve of antireflection coating during the irradiation of a laser pulse. The solid line shows the transmittance, the dashed line shows the laser pulse with a Gaussian shape. It is clear that the transmittance has dropped from the normal value of 0.96 to the abnormal value of 0.01. The decrease of transmittance is caused by the increase of the imaginary part of complex index. Consequently, the antireflection coating cannot work effectively before being damaged. In addition, the transmittance decreases, while the reflectivity and absorptivity increase. The transmittance is greater than the reflectivity in the first 120 femtoseconds. The standing wave pattern in the 33-layer stack is similar to the standing wave pattern in conventional antireflection coating (the maximum of electric filed is inside the stack). The transmittance is less than the reflectivity after 120 femtoseconds. The standing wave pattern in the 33-layer stack is similar to the standing wave pattern in high-reflection coating (the position of maximum of electric filed is located at the air/film interface).The variations of

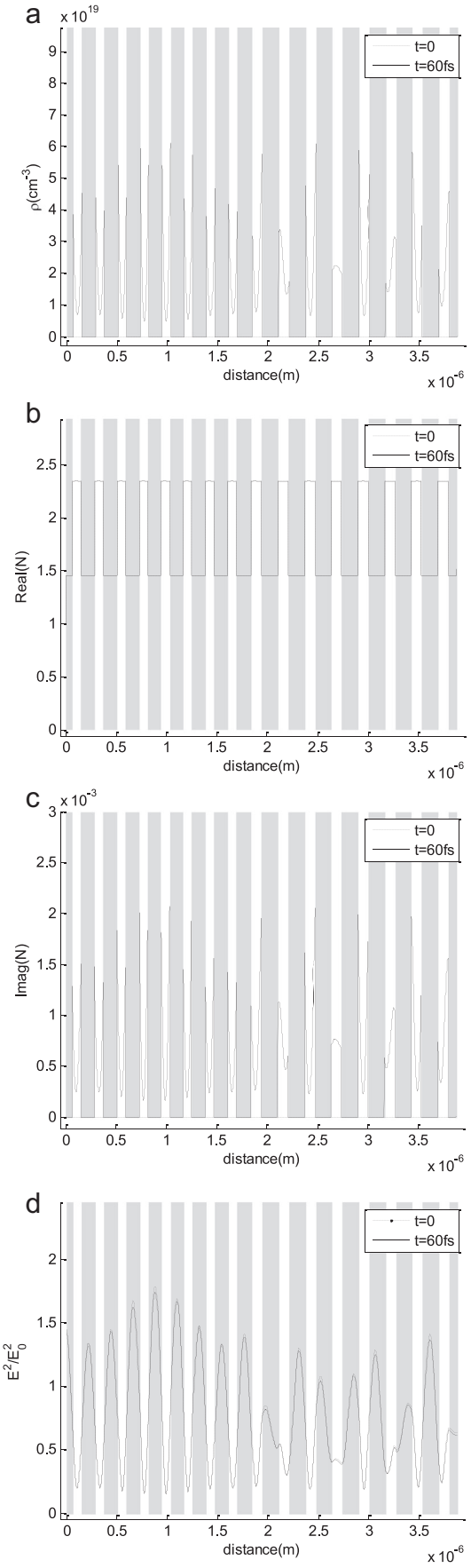

Fig.3. The spatial distributions of parameters in antireflection coating with irradiation time of 0 (dotted line),60 fs (solid line),respectively (a) the free electron density (ρ), (b) the real part of the complex index (N), (c) the imaginary part of the complex index (N), (d) the normalized electric field intensity ($E^2/E_0{}^2$).

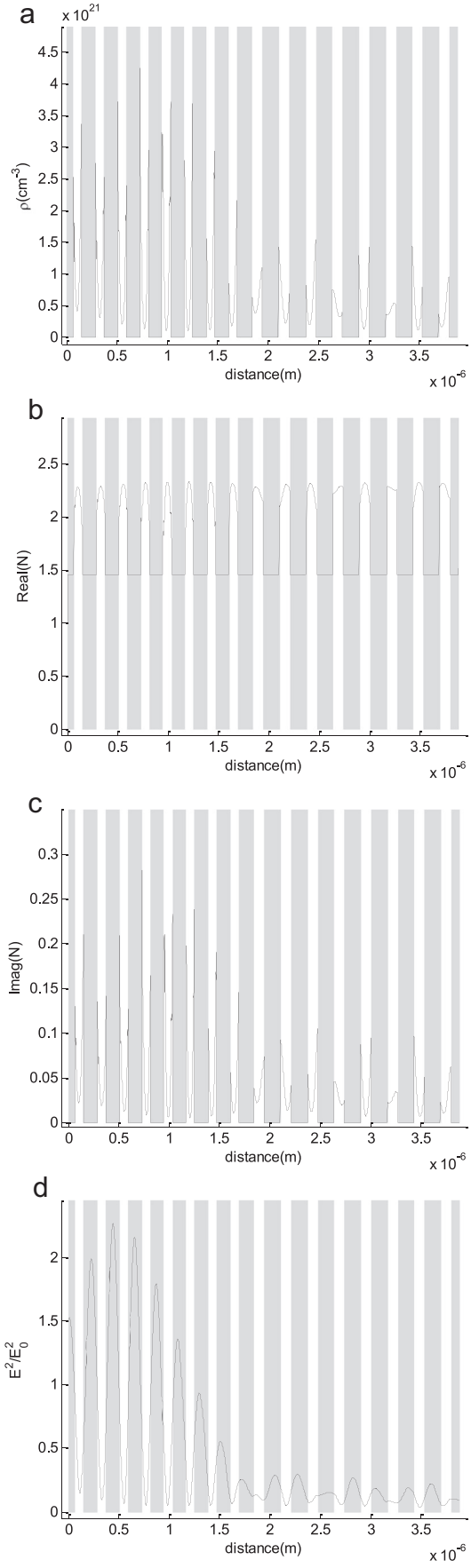

Fig.4. The spatial distributions of parameters in antireflection coating with irradiation time of 100 fs (a) the free electron density(ρ), (b) the real part of the complex index (N), (c) the imaginary part of the complex index (N), (d) the normalized electric field intensity($E^2/E_0{}^2$).

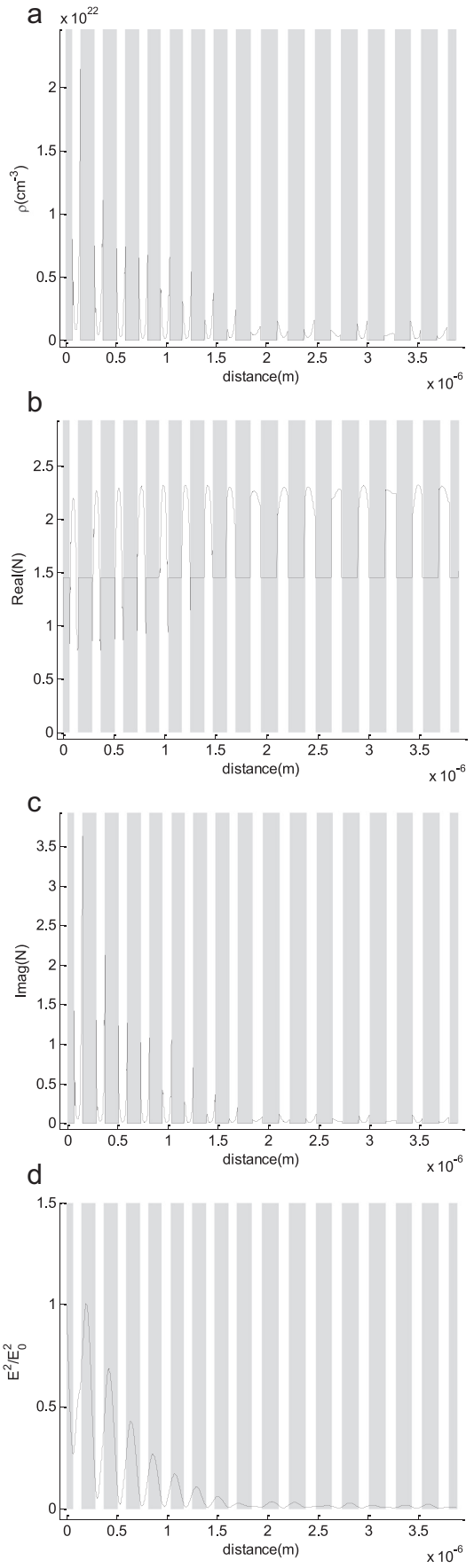

Fig.5. The spatial distributions of parameters in antireflection coating with irradiation time of 140 fs, (a) the free electron density(ρ), (b) the real part of the complex index (N), (c) the imaginary part of the complex index (N), (d) the normalized electric field intensity (E^2/E_0^2).

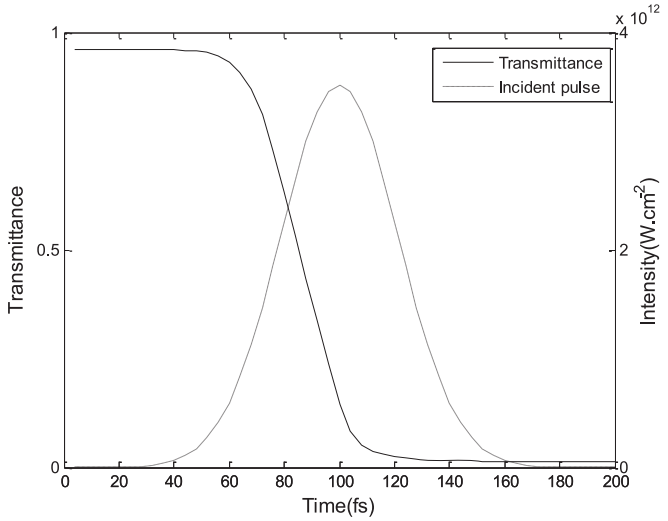

Fig. 6. The transmittance curve of antireflection coating.

transmittance and reflectivity could explain why the position of maximum of electric filed moves to the air/film interface, and why the position of maximum of free electron density moves to the air/film interface.

4. Conclusions

Based on the ionization theory and the correction theory of refractive index, a transient damage model of multilayer coating irradiated by ultrashort laser pulses is established. Specifically, the damage characteristics of an antireflection coating designed by ZnS/SiO_2 materials are calculated with ultra-short pulse irradiation.

Calculations combined with the correction theory of refractive index show that a coupling relationship exists between the refractive index, the electric field and the free electron density during the laser-film interaction process. The coupling process can be described as: With the increase of the free electron density, the real part of the refractive index decreases while the imaginary part increases. These changes will lead to modifications of the electric field repartition, which will further lead to the modification of the free electron density.

If the coupling process is not taken into consideration, the maximum of free electron density is located in Layer 25 by the theoretical calculation. Actually, in the coupling process, the electric field repartition leads the position of the maximum of free electron density to move toward the air/film interfaces. Ultimately, the free electron density achieves the critical damage value in the Layer 33, which means the damage has occurred in this layer.

In addition, the change of refractive index in the coupling process leads to the variation in the transmittance of antireflection coating. The transmittance has dropped from the normal value of 0.96 to the abnormal value of 0.01. Consequently, the antireflection coating cannot work effectively before being damaged.

The established model can help to carry out the transient analysis of related parameters in multilayer. And these works will contribute to a better understanding of the damage behavior.

References

[1] D. Du, X. Liu, G. Korn, J. Squier, G. Mourou, Laser-induced breakdown by impact ionization in SiO_2 with pulsewidths from 7 ns to 150 fs, Appl. Phys. Lett.

64 (1995) 3071–3073.
[2] B.C. Stuart, M.D. Feit, A.M. Rubenchik, B.W. Shore, M.D. Perry, Laser-induced damage in dielectrics with nanosecond to subpicosecond pulses, Phys. Rev. Lett. 74 (1995) 2248.
[3] B.C. Stuart, M.D. Feit, S. Herman, A.M. Rubenchik, B.W. Shore, M.D. Perry, Nanosecond-to-femtosecond laser-induced breakdown in dielectrics, Phys. Rev. B 53 (1996) 1749.
[4] J. Jasapara, A.V.V. Nampoothiri, W. Rudolph, Femtosecond laser pulse induced breakdown in dielectric thin films, Phys. Rev. B 63 (2001) 045117.
[5] X. Jing, J. Shao, J. Zhang, Y. Jin, H. He, Z. Fan, Calculation of femtosecond pulse laser induced damage threshold for broadband antireflective microstructure arrays, Opt. Express 17 (2009) 24137–24152.
[6] S. Chen, Y. Zhao, H. He, J. Shao, Effect of standing-wave field distribution on femosecond laser-induced damage of HfO_2/SiO_2 mirror coating, Chin. Opt. Lett. (2011), http://dx.doi.org/10.3788/COL201109.083101.
[7] G. Abromavicius, R. Buzelis, R. Drazdys, A. Melninkaitis, V. Sirutkaitis, Influence of electric field distribution on laser induced damage threshold and morphology of high reflectance optical coatings, Proc. SPIE 6720 (2007) 67200Y.
[8] L. Yuan, Y. Zhao, G. Shang, C. Wang, H. He, J. Shao, Z. Fan, Comparison of femtosecond and nanosecond laser-induced damage in HfO_2 single-layer film and HfO_2–SiO_2 high reflector, J. Opt. Soc. Am. B 24 (2007) 538–543.
[9] Benoît Laurent Gallais, Mireille Mangote, Andrius Commandré, Julius Melninkaitis, Maksim Mirauskas, Jeskevic, Valdas Sirutkaitis, Transient interference implications on the subpicosecond laser damage of multidielectrics, Appl. Phys. Lett. 97 (2010) 051112.
[10] T.Q. Jia, H.Y. Sun, X.X. Li, D.H. Feng, C.B. Li, S.Z. Xu, R.X. Li, Z.Z. Xu, H. Kuroda, The ultrafast excitation processes in femtosecond laser-induced damage in dielectric omnidirectional reflectors, J. Appl. Phys. 100 (2006) 023103.
[11] S. Chen, Y. Zhao, Z. Yu, Z. Fang, D. Li, H. He, J. Shao, Femtosecond laser-induced damage of HfO_2/SiO_2 mirror with different stack structure, Appl. Opt. 51 (2012) 6188–6195.
[12] C. Zhang, B. Fu, D. Zhang, F. Luo, The temperature disciplinarian of the ZnS/SiO_2/K9 filter under the 532 nm repetitive pulse laser, Appl. Laser 6 (2008) 017.
[13] F. Li, G. Liu, L. Du, R. Zhang, Comparisons and analyses of the properties of laser-induced damage to SiO_2 and ZnS, J. Mod. Optic. 61 (2014) 1158–1163.
[14] A. Vaidyanathan, T. Walker, A.H. Guenther, The relative roles of avalanche multiplication and multiphoton absorption in laser-induced damage of dielectrics, IEEE J. Quantum Electron. 16 (1980) 89–93.
[15] W.W. Thomas, H.G. Arthur, Pulsed laser-induced damage to thin-film optical coatings-Part II: theory, IEEE J. Quantum Electron. 17 (1981) 2053–2065.
[16] M. Mansuripur, G.A. Connell, J.W. Goodman, Laser-induced local heating of multilayers, Appl. Opt. 21 (1982) 1106–1114.
[17] N. Bloembergen, Laser-induced electric breakdown in solids, IEEE J. Quantum Electron. 10 (1974) 375–386.
[18] L. Wang, B. Fan, Z. Wang, Dielectric optical property transformation under irradiation of ultra-short pulse laser, Opt. Instrum. 30 (2008) 73–76.
[19] P.K. Kennedy, A first-order model for computation of laser-induced breakdown thresholds in ocular and aqueous media: Part I-theory, IEEE J. Quantum Electron. 31 (1995) 2241–2249.
[20] H. Sun, T. Jia, Z. Wei, et al., Dynamics of femtosecond laser pulse induced damage in multilayers, Opt. Mater. 28 (2006) 1372–1376.